Journal of Engineering and Applied Sciences 13 (Special Issue 13): 10687-10696, 2018
ISSN: 1816-949X

Demonstrate of Magnetic Field Effect on the Capability of Adsorption Process in the Removal of Azo Dye from the Aqueous Solutions on Calcined Iraqi Bentonite Clay Mineral via. Column Method

Mohammed H. Abdul Latif, Ibtisam J. Dawood, Basima Abdul Hassin Zaidan and Amer Jabber Jarad
Department of Chemistry, College of Education for Pure Science-Ibn Al-Haitham,
University of Baghdad, Baghdad, Iraq

Abstract: This study aims at the comparison to highlight the adsorption of [4-(hydroxyl-3, 5-dimethyl-phenyl azo) benzoic acid] azo dye ligand from aqueous solutions on calcined granulated initiated bentonite clay surface via. columnar method with and without the influence of magnetic field of 150 gauss field strength using super neodymium magnets. BET, Freundlich and Frumkin adsorption isotherms have been verified by using adsorption data. All experiments were done at different pH values (5.5, 7 and 8) using buffer solutions with a flow rate of 3 drops/min, at (25±2°C). A highest removal rate for azo ligand was (100% with magnetic field) and (92.857% without magnetic field) at pH 5.5. BET multi-layer isotherm is fitted well to the adsorption process of azo ligand under magnetic field in acidic media. Adsorption kinetic data obeys pseudo-second-order rate equations.

Key words: Magnetic field, dye removal, bentonite clay, columnar, mineral, magnetic

INTRODUCTION

The single largest chemical class industrial colorants are azo compounds (Mohammed *et al*., 2015). Azo dyes fall in the category of most reactive dyes. Azo dyes can contain one or more rarely azo groups and called (dis azo) (tris azo) (tetrakis azo) or (poly azo). The azo group is attached to two alkyl or aryl groups, more usually both of them are aryl groups (Siegrist *et al*., 1991). Exceptionally lightfast colors are obtained with metal-complexed azo dyes (Hunger, 2003). Decolorization of dyes is an important aspect of wastewater treatment (Panic *et al*., 2013). Wastewater pollution by dyes is a serious threat to the aquatic ecosystem which affects the quality of life and human health as well. Among the unwanted properties of dyes, resistance to natural degradation, allergenicity, carcinogenity and mutagenicity are all significant. They can also cause severe damage to human beings such as dysfunction of kidneys, reproductive system, liver, brain and central nervous system (Kadirvelu *et al*., 2003; Dinçer *et al*., 2007; Shen *et al*., 2009; Duruibe *et al*., 2007). Main technologies for treatment of dye-containing effluents were: ion exchange, adsorption, precipitation, biodegradation, membrane filtration, coagulation, flocculation, etc. A simple cost and effective technique used to degrade dyes is photo catalysis method. Dyes removal using adsorption techniques is widely used because of low cost processes (Tara-Lunga-Mihali *et al*., 2015). Activated carbon was widely used as adsorbent due to its high dyes sorption capacity but always we are looking for low-cost sorbents (Sanghi and Bhattacharya, 2002). Natural clays are low cost materials with good adsorption ability due to their great surface area, chemical stability, layered structure and high Cation Exchange Capacity (CEC). Natural widespread bentonite clay minerals is a cheap material used as an alternative material for the removal of azo dyes from wastewater effluents (Khenifi *et al*., 2007; Mellah and Chegrouche, 1997; Naseem and Tahir, 2001; Hashemian, 2007). Bentonite of West Iraq (Traifawi) has a great particles surface area, estimated using Methylene Blue (MB) adsorption method which was (123 m^2/g). Mostly Bentonite consists of Ca^{+2} montmorillonite clay mineral with (60-65%) montmorillonite of crude bentonite, so, it is important to remove impurities before use (Latif *et al*., 2013). This study is a comparative study aimed to evaluate the efficiency of adsorption of 4-(hydroxyl-3, 5 dimethyl-phenyl azo)-benzoic acid azo dye prepared by coupling the diazonium salts of amines with 2, 4 dimethylphenol (Jarad and Kadhim, 2015) on the surface of Iraqi activated calcined granulated bentonite clay mineral packed in glass columns with and without the influence of a magnetic field, calculating the effect of many variables like pH, ionic strength, contact time, clay

Corresponding Author: Mohammed H. Abdul Latif, Department of Chemistry,
College of Education for Pure Science-Ibn Al-Haitham, University of Baghdad, Baghdad, Iraq

weight on the % removal of azo ligand and the isothermic factors of adsorption processes. The adsorptive tests at both presence and absence of the magnetic field were performed.

MATERIALS AND METHODS

Chemicals and raw materials: All chemicals and solvents were analytical grade (supplied by Merck and Fluka). Distilled water was used in experiments with measured conductivity (1.5×10^{-5} S cm^{-1}). Bentonite of West Iraq (Traifawi) with known chemical components was supplied by Geological Survey and Mining General Company Baghdad, Iraq (Latif *et al*., 2013). Samples were sieved to a desired particle size (45 μm), dried for 24 h at 110°C in electrical oven and stored in a desiccator before use.

Azo ligand and clay mineral preparation and beneficiation: Preparation procedure for the of 4 (hydroxyl- 3, 5-dimethyl-phenyl azo)-benzoic acid azo dye ligand was applied by (Amer Jabber Jarad) as shown in Fig. 1 (Jarad and Kadhim, 2015).

Also, the preparation of buffer and stock solutions was done, respectively (Robinson and Stokes, 1968) and using bentonite of West Iraq (Traifawi) a granulated calcined initiated Na montmorillonite clay mineral was synthesized and characterized by Fourier FT-IR spectroscopic analysis (Shimadzu FTIR spectrometer-30 000:1/IRAff), X-Ray Diffraction (XRD) on Shimadzu X-ray diffraction P 04-XRD-6000 and SEM micrographs were carried out on VEGA3-TESCAN scanning electron microscope (Latif, 2015).

Column adsorption method: Three standard 30 ppm concentration solutions of azo dye were prepared using stock solutions of different pH (5.5, 7 and 8). Using (UV-1800 Shimadzu spectrophotometer) the UV-Visible spectrum has been recorded, showing that the maximum absorption wavelength values (λ_{max}) was (339 nm at pH 5.5) (340 nm at pH 7) and (342 nm at pH 8), respectively.

At a range of (5-30 mg/L) concentration we prepare six standard solutions of azo ligand from the stock solutions of azo ligand of different pH (5.5, 7 and 8). Then we measure the absorbance of each solution at (λ_{max}) against blank consist of a buffer solution corresponding to its pH value. Three calibration curves were plotted between absorbance and azo ligand standard solutions concentrations as shown in Fig. 1-3, respectively.

A constant weight (1 g) of clay adsorption bed (granulated initiated calcined na-montmorillonite) was

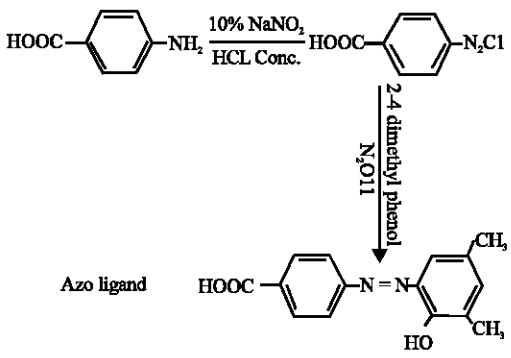

Fig. 1: Schematic representation of synthesis of 4-(2-hydroxy-3, 5-dimethlyl-phenyl azo)-benzoic acid

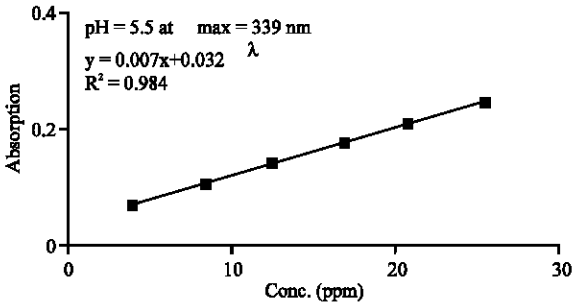

Fig. 2: A calibration curve of azo ligand with buffer soln pH = 5.5 at λ_{max} = 339 nm

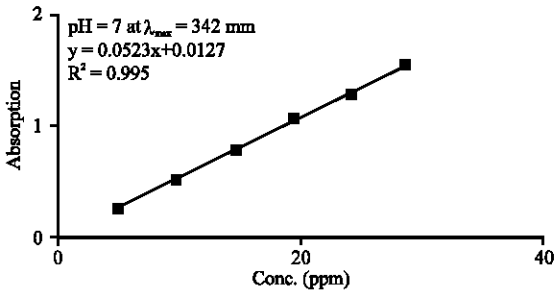

Fig. 3: A calibration curve of azo ligand with buffer soln. pH = 7 at λ_{max} = 340 nm

transferred to each of 12 glass columns (50 cm*10 mm i.d) to have a bed height of (17 mm). Also, the surface area of the (1 g) granulated clay bed was calculated physically to be (23.904 cm^2). Six of these columns have been prepared and surrounded by magnetic field of (150 gauss field strength using super neodymium magnets) to flow (10 mL) of (20-70 mg/L) azo ligand solutions of different pH level (5.5, 7 and 8) at (3 drops/min) flow rate and (25±2°C) once without and the other under magnetic field.

Table 1: Adsorption data of azo ligand on activated, calcined and granulated west Iraq montmorillonite clay mineral

Concentration of azo dye (°C ppm)	At pH 5.5 λ_{max} = 339 nm				At pH 7 λ_{max} = 340 nm				At pH 8 λ_{max} = 342 nm			
	Absorption	C_e (ppm)	Removal (%)	q_e	Absorption	C_e	Removal (%)	q_e	Absorption	C_e (ppm)	Removal (%)	q_e
Adsorption data of azo ligand on bentonite clay mineral packed in six columns without magnetic field												
20	0.064	4.5714	77.143	0.1543	0.235	4.2504	78.748	0.1575	0.269	4.6320	76.84	0.15368
30	0.070	5.4285	81.900	0.2457	0.459	8.5334	71.555	0.2146	0.367	6.3573	78.81	0.16643
40	0.069	5.2857	86.785	0.3471	0.965	18.0363	54.909	0.2196	1.073	18.7869	53.30	0.21213
50	0.069	5.2857	89.428	0.4471	1.403	26.5831	46.833	0.2341	1.570	27.5397	44.92	0.22460
60	0.062	4.2857	92.857	0.5571	0.901	16.9847	71.169	0.4301	0.711	12.4137	79.31	0.47586
70	0.112	11.4280	83.674	0.5857	1.757	33.3518	52.354	0.3664	2.061	36.1813	48.31	0.33819
Adsorption data of azo ligand on bentonite clay mineral packed in six columns under magnetic field (150 Gauss)												
20	0.010	0.0000	100	0.2000	0.149	2.6061	86.969	0.1739	0.365	6.3222	68.39	0.13678
30	0.005	0.0000	100	0.3000	0.247	4.4799	85.506	0.2552	0.611	10.6531	64.45	0.19347
40	0.028	0.0000	100	0.4000	0.802	15.0917	62.270	0.2491	1.143	20.0193	49.95	0.19981
50	0.014	0.0000	100	0.5000	1.083	20.4646	59.071	0.2953	1.721	30.1954	39.61	0.19805
60	0.035	0.4285	99.2858	0.5957	0.385	7.1854	88.024	0.0835	1.453	25.4771	57.54	0.34523
70	0.048	2.2857	96.7347	0.6771	1.713	32.5105	53.556	0.3749	2.641	46.3926	33.72	0.23607

(q_e): Adsorbed amount ($q_e = (C_0-C_e)V/W$ (mg adsorbate/g adsorbent)) and removal % = 100($C_0-C_e)/C_0$ (C_0: Initial Conc. of sorbate mg/L, C_e: Equilibrium adsorbate concentration mg/L, V: Volume of solution in liter and w: Adsorbent mass in grams) (Zlem and Demet, 2000)

The absorbance of percolated solutions was measured at (λ_{max}) for each pH level using (UV-Vis-1800 Shimadzu spectrophotometer). Equilibrium adsorption uptake and (%) removal of azo ligand from the aqueous solution q_e (mg/g) was calculated (Table 1) (Zlem and Demet, 2000).

RESULTS AND DISCUSSION

Calibration curves: A three linear calibration curves for azo ligand was obtained at different pH (5.5, 7 and 8) (Fig. 1-3) which obey Beer's law at a concentration range of 5-30 mg L^{-1}. Coefficient of determination (R^2), Limit of Detection LOD and other parameters were given in (Table 2).

Azo ligand initial concentration (°C) and pH effect: Plotting (°C) values via. azo ligand removal % to study the effect of °C on a fixed (1 g) activated calcined and granulated clay bed with and without magnetic field at different pH (5.5, 7 and 8) buffer solutions and at (25±2°C) as shown in Fig. 4-6.

When we take a look to the graphs we see that the highest azo ligand adsorption is at acidic media (pH 5.5) due to the acidic character of azo ligand and the increase in azo ligand initial concentration increase the removal percent to a maximum adsorption capacity of the clay bed at (Co = 60 ppm) without magnetic field and (Co = 50 ppm) with magnetic field. Also, we find that the highest azo ligand adsorption occurs with magnetic field at acidic and neutral media (pH: 5.5 and 4) (Fig. 5 and 6) due to positive impact of magnetic field azo ligand molecules exist in acidic and neutral media leading to increment of azo molecules mobility which increase the adsorption ability. Whereas at alkaline media (pH 8) (Fig. 7) we find that the highest azo ligand adsorption happen without magnetic field due to the negative impact of magnetic field on the azo ligand molecules in alkaline media. Effect of pH on azo

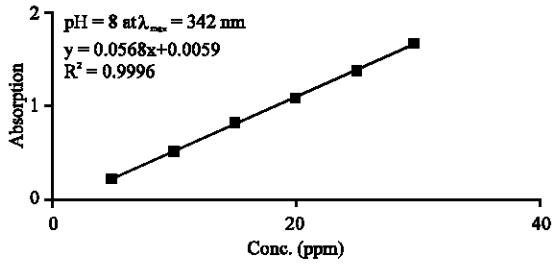

Fig. 4: A calibration curve of azo ligand with a buffer soln. pH = 8 at λ_{max} = 342 nm

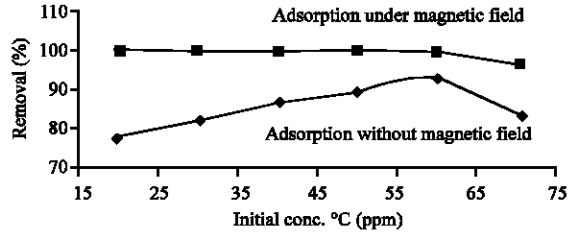

Fig. 5: Initial conc. °C effect at pH = 5.5

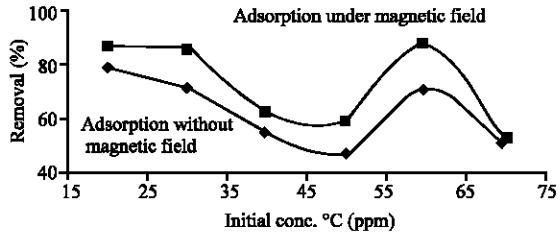

Fig. 6: Initial conc. °C effect at pH = 7

Table 2: Regression equation statistical data and spectral characterization of azo ligand adsorption on activated calcined and granulated Iraqi montmorillonite clay mineral

	Azo ligand		
Parameters	pH 5.5 λ_{max} = 339 nm	pH 7 λ_{max} = 340 nm	pH 8 λ_{max} = 342 nm
Range of linearity (ppm)	5-30	5-30	5-30
Equation of regression			
Intercept	0.03200	0.012667	0.005867
Intercept standard deviation	0.008722	0.032389	0.011650
Slope	0.007029	0.052314	0.056846
Slope standard deviation	0.000448	0.001663	0.000598
Coefficient of determination R^2	0.984013	0.995973	0.999557
Estimation standard error	0.009369	0.034791	0.012514
The F statistic	246.2002	989.2089	9027.522
The regression sum of squares	0.021613	1.197343	1.413753
The residual sum of squares	0.000351	0.004842	0.000626
Degree of freedom	4	4	4
Y and X axis standard error STEYX	0.009369	0.034791	0.012514
Limit of detection (sensitivity) LOD	4.398591	2.194681	0.726457
Limit of quantitation LOQ	13.329065	6.650418	2.201386

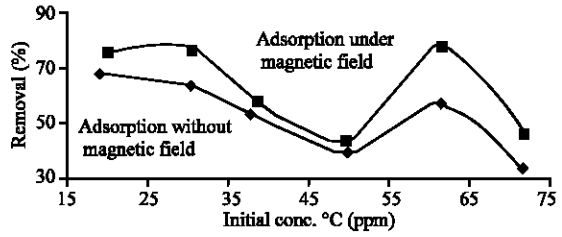

Fig. 7: Initial conc. °C effect at pH = 8

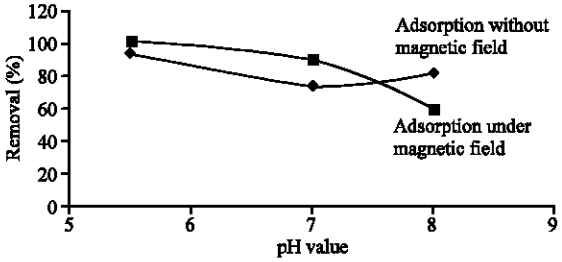

Fig. 8: Effect of pH on adsorption removal % of azo ligand with and without magnetic field, C = 60 ppm

ligand adsorption removal % with and without magnetic field was shown clearly in Fig. 7 at which the highest adsorption happen at acidic media (pH: 5.5), therefore, we see that it is important to study the effect of pH at acidic media on adsorption to now highest adsorption acidic media of azo ligand. A seven azo ligand solutions of constant concentration (60 ppm without magnetic field and 50 ppm with magnetic field) adjusted to different pH values (2.5, 3.0, 3.5, 4.0 4.5, 5.0 and 5.5). Then flowing (10 mL) of each solution through a three columns of 1 g clay bed at a constant (3 drops/min) flow rate at (25±2°C) once with and without magnetic field. The flowing solutions were examined by measuring the absorbance at (λ_{max}) for each pH level using (UV-Vis-1800 Shimadzu

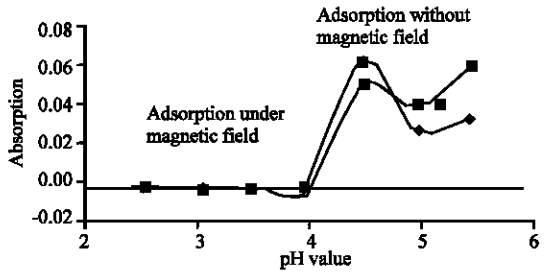

Fig. 9: Effect of pH at acidic media on adsorption of azo ligand with and without magnetic field

spectrophotometer). The absorbance of these solutions was measured at each (λ_{max}) after flowing through adsorption columns then plotting absorbance against the pH values, Fig. 8 shows that the absorbance increases (i.e., adsorption removal % increased) when the acidity increased with and without magnetic field.

Weight effect of column adsorption bed: Seven column of different clay bed weights ranged from (1-2.2 g) were prepared for flowing (10 mL) of azo ligand solutions of (60 ppm) concentration without magnetic field and (50 ppm) concentration with magnetic field at study rate of flow (3 drops/min) at (25±2°C). The absorbance of these solutions were measured after flowing through the columns then removal % was calculated and plotting removal % of azo ligand against clay weight as shown in Fig. 9 and 10. The graphs show that the highest adsorption of azo ligand without magnetic field was on clay bed of 1.8 g (Fig. 9). This indicates that azo ligand absorption increased with increasing of clay weight to an upper limit of clay capacity and bed surface area. While the adsorption with the presence of a magnetic field (Fig. 10) gives high values fixed with all clay weights.

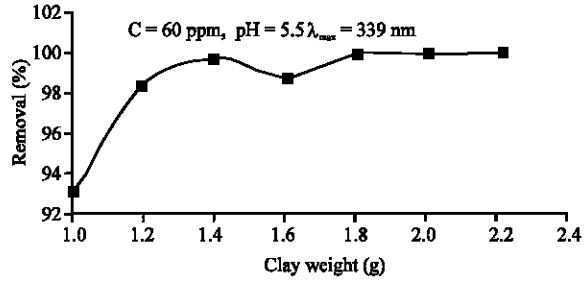

Fig. 10: Effect of column clay bed weight on azo ligand adsorption without magnetic field

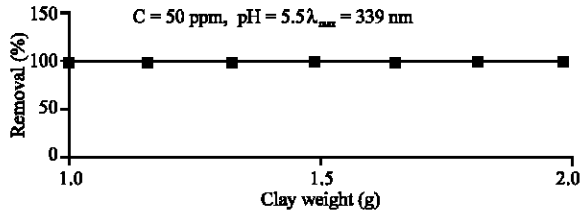

Fig. 11: Effect of column clay bed weight on azo ligand adsorption with magnetic field

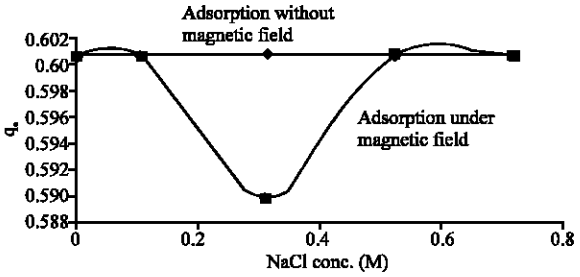

Fig. 12: Effect of solutions ionic strength on adsorption of azo ligand on calcined montmorillonite with and without magnetic field (C = 60 ppm without magnetic field and C = 50 ppm with magnetic field), pH = 5.5, clay wt. = 1.8 g and λ_{max} = 339 nm

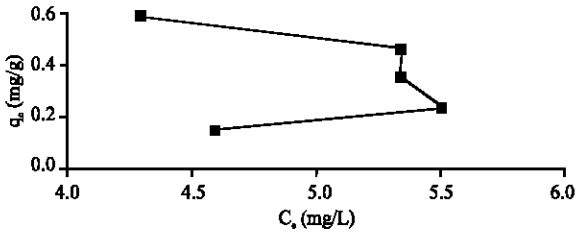

Fig. 13: Adsorption isotherm of azo ligand without magnetic field at pH = 5.5

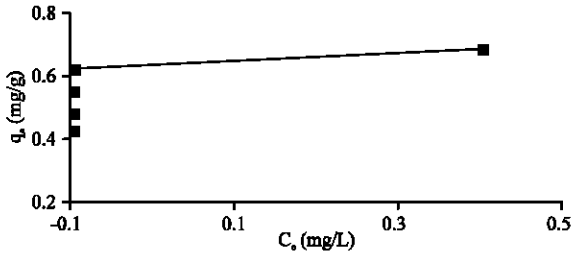

Fig. 14: Adsorption isotherm of azo ligand with magnetic field at pH = 5.5

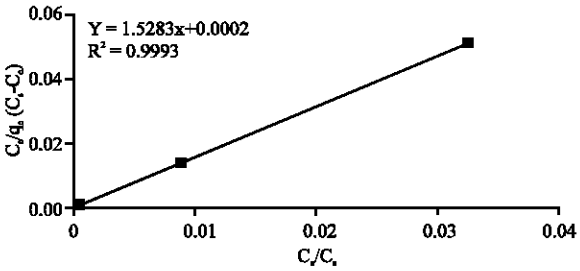

Fig. 15: Bet linear adsorption isotherm with magnetic field

Effect of solutions Ionic strength: To study the ionic strength factors, a five different sodium chloride solutions (0.0, 0.1, 0.3, 0.5 and 0.7 M) was added to three (10) mL azo ligand solutions of concentration (60 ppm without magnetic field and 50 ppm with magnetic field). The absorbance of these solutions was measured after flowing through four adsorption columns of 1.8 g clay bed with and without magnetic field. (q_e) was calculated and drawing (q_e) against the Na^+ and Cl^- solutions concentrations (Fig. 11). The graph show a constant maximum adsorption (without magnetic field) with increasing of Na^+ and Cl^- ions concentration on the clay bed surface and that is because of the high electrostatic interaction of these ions with the azo ligand and slight decrease in adsorption (with magnetic field) at 0.3 M NaCl concentration due to ion pair formation with Cl^- ions that reduce the impact of magnetic field and lower the adsorption ability.

Adsorption isotherms: Adsorption data are usually described by adsorption isotherms (mathematical models that describe the distribution of the adsorbate species among liquid and adsorbent bed) such as BET, Freundlich and Frumkin isotherms (Zlem and Demet, 2000; Agarwal *et al*., 2014). Experimental results of azo ligand adsorption at (pH 5.5) with and without magnetic field as presented in Table 3 were fitted with the BET, Freundlich and Frumkin Models (Fig. 12-19).

The BET isotherm (multilayer adsorption): BET isotherm is an important isotherm type describes multi-layer sorption was developed by Brunauer *et al.* (1938). The BET isotherm model in the linear form as used in the present study is represented as:

Table 3: Adsorption isotherms experimental data, pH 5.5, λ_{max} = 339 nm

				BET		Freundlich		Frumkin	
C_s	q_e	C_e (ppm)	Removal (%)	C_e/C_s	C_e/q_e (Cs-Ce)	Log q_e	Log C_e	C_o	*Θ/1-Θ
Experimental data of the adsorption isotherms without magnetic field, pH 5.5, λ_{max} = 339 nm									
20	0.1543	4.5714	77.143	0.22857	1.9202	-0.8116	0.6600	20	-0.1515
30	0.2457	5.4285	81.900	0.18095	1.4318	-0.6096	0.7201	30	-0.1286
40	0.3471	5.2857	86.785	0.13214	0.4386	-0.4695	0.7231	40	-0.0967
50	0.4471	5.2857	89.428	0.10571	0.2644	-0.3496	0.7231	50	-0.0789
60	0.5571	4.2857	92.857	0.07193	0.1808	-0.2541	0.6320	60	-0.0519
70	0.5857	11.4280	83.674	0.16325	0.3331	-0.2323	1.0579	70	-0.1296
Experimental data of the adsorption isotherms with magnetic field, pH 5.5, λ_{max} = 339 nm									
20	0.2000	0.0000	100	0.0000	0	-0.6989	0.0000	20	0.0526
30	0.3000	0.0000	100	0.0000	0	-0.5228	0.0000	30	0.0344
40	0.4000	0.0000	100	0.0000	0	-0.3979	0.0000	40	0.0256
50	0.5000	0.0000	100	0.0000	0	-0.3010	0.0000	50	0.0204
60	0.5957	0.4285	99.2858	0.0071	0.0121	-0.2249	-0.3680	60	0.0095
70	0.6771	2.2857	96.7347	0.0326	0.0498	-0.1693	0.3590	70	-0.0183

*Θ = 1-C_e/C_o

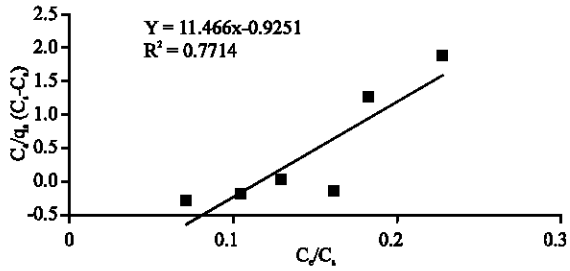

Fig. 16: Bet linear adsorption isotherm without magnetic field

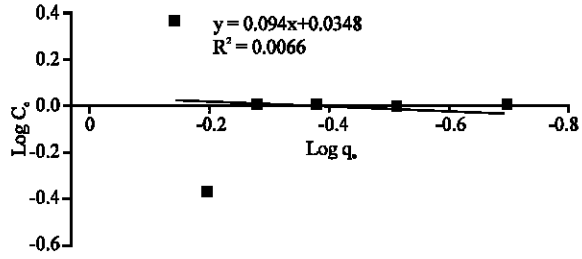

Fig. 17: Freundlich linear adsorption isotherm of azo ligand with magnetic field

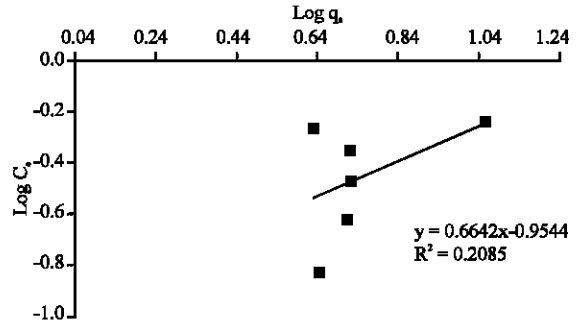

Fig. 18: Freundlich linear adsorption isotherm of azo ligand without magnetic field

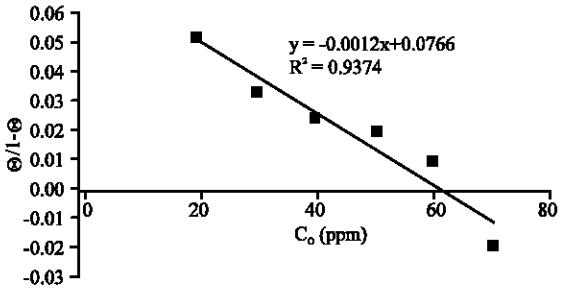

Fig. 19: Frumkin linear adsorption isotherm of azo ligand with magnetic field

$$\frac{C_e}{q_e(C_e-C_s)} = \frac{1}{q_s\,CBET} + \frac{CBET-1}{q_s\,CBET}\left(\frac{C_e}{C_s}\right)$$

Where:

C_e = Equilibrium concentration (mg/L)

C_s = Adsorbate monolayer saturation concentration (mg/L)

CBET = BET adsorption isotherm relating to the energy of surface interaction (L/mg)

The ability of BET Model to fit the experimental data was examined by plotting C_e/q_e (C_s-C_e) vs. C_e/C_s with and without magnetic field (Fig. 14 and 15) (Agarwal *et al*., 2014). BET isotherm was fitted well with a coefficient of determination (R^2 = 0.9993) and (R^2 = 0.7714) with and without magnetic field, respectively. BET equation assumes that:

- The adsorption occurs layer by layer
- The first layer molecules interact with the solid and molecules in the following layers, behave as in the bulk liquid
- The lateral interactions between adsorbed molecules are neglected
- Langmuir theory can be applied to each layer

Freundlich isotherm: Freundlich isotherm is an empirical relationship describing the adsorption of solutes from a liquid to a solid surface assuming that different sites with several adsorption energies are involved (Agyei *et al*., 2000; Baup *et al*., 2000). Freundlich adsorption isotherm is the relationship between the amounts of ligand adsorbed per unit mass of adsorbent q_e and the concentration of the azo ligand at equilibrium, C_e. The logarithmic form of the equation becomes:

$$q_e = K_f C_e^{1/n}$$

The linear equation of Freundlich Model can be represented as follows:

$$\text{Log}\, q_e = \text{Log}\, K_f + T/\text{Log}\, C_e$$

where, K_f and n are the Freundlich constants, the characteristics of the system K_f and n are the indicators of the adsorption capacity and adsorption intensity, respectively. The ability of Freundlich Model to fit the experimental data was examined by plotting log C_e vs. log q_e with and without magnetic field to generate the intercept values of K_f and the slope of n from (Fig. 16 and 17). Freundlich constants were found to be (K_f = 0.034773, n = 0.0.094019) with magnetic field and (K_f = -0.95442, n = 0.664229) without magnetic field. Freundlich isotherm was fitted with a coefficient of determination (R^2 = 0.0066) and (R^2 = 0.2083) with and without magnetic field.

Frumkin adsorption isotherm: Frumkin adsorption isotherm is a three-parameter model. According to this model, the bulk solution is ideal but the adsorbed monolayer is not ideal. It allows for the interactions between the adsorbed surfactant molecules. The interactions occur only between the neighbor adsorbed surfactant molecules in the monolayer in a pair-wise manner (Prosser and Franses, 2001). Frumkin adsorption isotherms were applied to describe the adsorption mechanism for azo ligand. The general form of Frumkin isotherm is:

$$f(\Theta, x)\exp.(-2\alpha\Theta) = KC$$

Where:

$f(\Theta, x)$ = The configurational factor which depends upon the physical model and assumptions underlying the derivative of the isotherm
Θ = The surface coverage
C = The azo ligand concentration
x = The size ratio
α = The molecular interaction parameter
K = The equilibrium constant of the adsorption process

The Frumkin adsorption isotherm can be expressed according to equation:

$$\text{Log}\left\{C\left(\frac{\Theta}{1-\Theta}\right)\right\} = 2.303\text{Log}\,K + 2\alpha\Theta$$

Where:

K = The adsorption-desorption constant
α = The lateral interaction term describing the interaction in the adsorbed layer

Plots of $\Theta/(1-\Theta)$ versus azo ligand Concentration (C) with and without magnetic field as presented in Fig. 18 and 19 are linear which shows the applicability of the Frumkin isotherm. Lateral interaction term (a) is calculated from the slope of the Frumkin isotherm, indicates the interaction between azo ligand molecules on the surface of calcined clay (Martinez and Stern, 2002). It was found to be (α = 0.0766) with magnetic field and (α = -0.1522) without magnetic field, respectively. Frumkin isotherm was fitted well with magnetic field (R^2 = 0.9374) and not fitted well without magnetic field (R^2 = 0.265). This indicate that the high inter between azo ligand molecules under magnetic field will increase the adsorption ability. BET, Freundlich and Frumkin adsorption constants and the coefficient of determination (R^2) with and without magnetic field are presented in Table 4.

From Table 4, we see that the multi-layer BET isotherm is fitted well to the adsorption process of azo ligand under magnetic field in acidic media due to high interaction between azo ligand molecules and high charge effect of clay adsorbate surface under the influence of magnetic field.

Flow rate (contact time) effect: The adsorption removal % of azo ligand was measured at five different flow rates for a solution of azo ligand (60) ppm, concentration without magnetic field, Fig. 20 shows that removal % of azo ligand was high at low rates then decreased due to access to the equilibrium adsorption time and increased again to reach 100% removal due to fast multi-layer adsorption. This is probably due to high contact time at these low flow rates. Table 5 show the calculated parameters that illustrate the importance of flow rate and contact time.

Adsorption kinetics: Rate of the adsorption process can be examined by kinetic models; Kinetic data obtained from the studies have been analyzed using

Table 4: Isotherm models constants and the coefficient of determination (R^2) of azo ligand with and without magnetic field

	Bet isotherm		Freundlich isotherm		Frumkin	
Adsorbent	R^2	K_f	N	R^2	α	R^2
Isotherm models constants and the coefficient of determination (R^2) of azo ligand with magnetic field						
Initiated burned Iraqi bentonite clay	0.9993	0.034773	0.00940190	0.0066	0.0766	0.9374
	0.7714	-0.954420	0.66422900	0.2083	-0.1522	0.2650

Table 5: Adsorption kinetic parameters of contact time effect on adsorption of 10 mL aqueous solution of (50 and 60 mg/L) azo ligand

Initial conc. (mg/L)	Flow rate (drop/min)	Flow rate (mL/min)	Time (min)	Equilibrium conc. (C_t) (mg/L)	Removal (%)	q_t (mg/g)	Ln (q_e-q_t)	t/q_t	Equilibrium time (min)
60	1	0.05	200.000	0.000	100.00	0.600		333.333	66.666
	2	0.10	100.000	6.857	88.57	0.531	-0.6496	188.324	
	3	0.15	66.666	4.285	92.86	0.557		119.687	
	4	0.20	50.000	0.000	100.00	0.600		83.333	
	5	0.25	40.000	0.000	100.00	0.600		66.666	
	6	0.30	33.333	0.000	100.00	0.600		55.555	

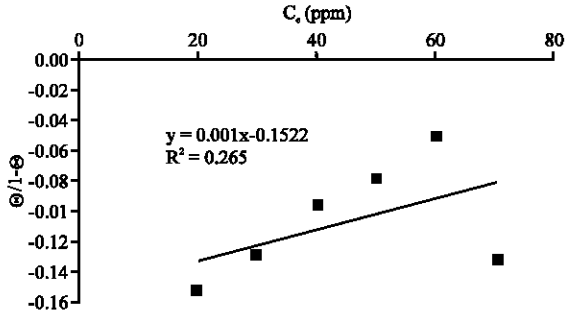

Fig. 20: Frumkin linear adsorption isotherm of azo ligand without magnetic field

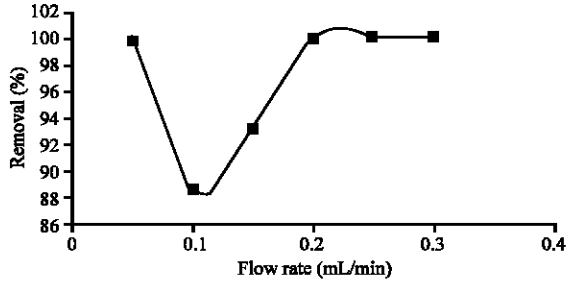

Fig. 21: Flow rate effect on the adsorption removal % of azo ligand (50 and 60) ppm, concentration with and without magnetic field, clay wt. = 1.8 g and pH = 5.5

pseudo-first-order and pseudo-second-order models. Lagergren first order equation is expressed as follows:

$$\frac{d_q}{d_t} = k_1(q_e - q_t)$$

Where:

q_e = The amount of azo ligand adsorbed at equilibrium (mg/g)

q_t = The amount of azo ligand adsorbed at time t (min^{-1})

k_1 = The rate constant of pseudo-first-order adsorption If it supposed that q = 0 at t = 0 then:

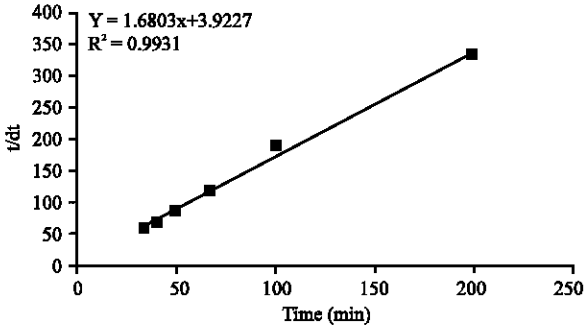

Fig. 22: Pseudo 2nd-order kinetic models of azo ligand adsorption of (60 ppm) aqueous solution at 25±2°C

$$\ln(q_e - q_t) = \ln q_e - k_1 t$$

The equation of pseudo-second-order kinetic rate is expressed as follows:

$$\frac{dq_t}{d_t} = k_2(q_e - q_t)^2$$

where, k_2 is the rate constant of pseudo-second-order sorption (g/mg/min). The integrated form of equation when ($t = 0 \rightarrow t$ and $q_t = 0 \rightarrow q_e$) the following expression is obtained:

$$\frac{t}{q_t} = \frac{1}{k_2 q_e^2} + \frac{t}{q_e}$$

After noting the results of Table 5, we found that we cannot plot the linear graph of the first order kinetic model. Therefore, azo ligand adsorption on calcined clay surface was well defined by the pseudo second order reaction kinetic. Also, plotting (t/q_t) against (t) should give a linear relationship with a slope of ($1/q_e$) and intercept of ($1/k_2 q_e^2$)(Fig. 21 and 22). Showing us that the

Table 6: Pseudo-second-order kinetic parameters for adsorption of azo ligand from 10 mL (60 ppm) aqueous solution at (25±2)°C

	The pseudo-second-order kinetic models		
q_e experimental (mg/g)	q_e calculated (mg/g)	K_2 (mg/g/min)	R^2
0.557	0.595	0.7201	0.9931

correlation coefficient of the second order reaction kinetic is high (R^2 = 0.5506). Table 6 shows the rate constants (q_e experimental and calculated) and correlation coefficient (R^2) for pseudo second order reaction kinetic.

CONCLUSION

This study indicates that the Iraqi initiated calcined bentonite clay mineral is an effective adsorbent for the removal of azo ligand from acidic aqueous solutions with and without magnetic field. Also, we find that the highest azo ligand adsorption occurs with magnetic field at acidic and neutral media (pH:5.5 and 7) due to positive impact of magnetic field azo ligand molecules exist in acidic and neutral media leading to increment of azo molecules mobility which increase the adsorption ability. Whereas at alkaline media (pH = 8) we find that the highest azo ligand adsorption happen without magnetic field due to The negative impact of magnetic field on the azo ligand molecules in alkaline media. The multi-layer BET isotherm is fitted well to the adsorption process of azo ligand under magnetic field in acidic media due to high interaction between azo ligand molecules and high charge effect of clay adsorbate surface under the influence of magnetic field. Adsorption of azo ligand obeys pseudo-second order equation with good correlation.

ACKNOWLEDGEMENT

We would like to acknowledge Chemistry Department of the College of Education for Pure Science Ibn Al-Haitham for their Financial support.

REFERENCES

Agarwal, A.K., M.S. Kadu, C.P. Pandhurnekar and I.L. Muthreja, 2014. Langmuir, Freundlich and BET adsorption isotherm studies for zinc ions onto coal fly ash. Intl. J. Appl. Innov. Eng. Manage., 3: 64-71.

Agyei, N.M., C.A. Strydom and J.H. Potgieter, 2000. An investigation of phosphate ion adsorption from aqueous solution by fly ash and slag. Cem. Concr. Res., 30: 823-826.

Baup, S., C. Jaffre, D. Wolbert and A. Laplanche, 2000. Adsorption of pesticides onto granular activated carbon: Determination of surface diffusivities using simple batch experiments. Adsorpt., 6: 219-228.

Brunauer, S., P.H. Emmett and E. Teller, 1938. Adsorption of gases in multimolecular layers. J. Am. Chem. Soc., 60: 309-319.

Dincer, A.R., Y. Gunes, N. Karakaya and E. Gunes, 2007. Comparison of activated carbon and bottom ash for removal of reactive dye from aqueous solution. Bioresour. Technol., 98: 834-839.

Duruibe, J.O., M.O.C. Ogwuegbu and J.N. Egwurugwu, 2007. Heavy metal pollution and human biotoxic effects. Int. J. Phys. Sci., 2: 112-118.

Hashemian, S., 2007. Study of adsorption of acid dye from aqueous solutions using bentonite. Main Group Chem., 6: 97-107.

Hunger, K., 2003. Industrial Dyes Chemistry: Properties, Applications. Wiley, Hoboken, New Jersey, USA., ISBN:9783527304264, Pages: 648.

Jarad, A.J. and Z.S. Kadhim, 2015. Synthesis, spectral, dyeing performance and biological activity studies of AZO dyes complexes with some metal ions. Intl. J. Human. Arts. Med. Sci., 3: 197-210.

Kadirvelu, K., M. Kavipriya, C. Karthika, M. Radhika and N. Vennilamani *et al*., 2003. Utilization of various agricultural wastes for activated carbon preparation and application for the removal of dyes and metal ions from aqueous solutions. Bioresou. Technol., 87: 129-132.

Khenifi, A., Z. Bouberka, F. Sekrane, M. Kameche and Z. Derriche, 2007. Adsorption study of an industrial dye by an organic clay. Adsorption, 13: 149-158.

Latif, M.H.A., 2015. Preparation and characterization for a new ZnO-Montmorillonite hybrid from Iraqi (Traifawi) Clay Minerals. Chem. Mater. Res., 7: 18-23.

Latif, M.H.A., T.H. Al-Noor and K.A. Sadiq, 2013. Adsorption study of symmetrical Schiff base ligand 4,4'-[hydrazine-1,2-diylidenebis (methan-1-yl-1-ylidene) bis(2-methoxyphenol)] on granulated initiated calcined Iraqi montmorillonite via columnar method. Adv. Phys. Theor. Applic., 24: 38-51.

Martinez, S. and I. Stern, 2002. Thermodynamic characterization of metal dissolution and inhibitor adsorption processes in the low carbon steel/mimosa tannin/sulfuric acid system. Appl. Surf. Sci., 199: 83-89.

Mellah, A. and S. Chegrouche, 1997. The removal of zinc from aqueous solutions by natural bentonite. Water Res., 31: 621-629.

Mohammed, H.J., M.A. Awad and S.H. Mallah, 2015. Preparation and characterization studies of manganese (II) complex with azo reagent (antipyriyl azo-1-nitroso-2-naphthol) by spectrophotometric methods. Inter. J. Basic Appl. Sci., 15: 25-33.

Naseem, R. and S.S. Tahir, 2001. Removal of Pb(II) from aqueous/acidic solutions by using bentonite as an adsorbent. Water Res., 35: 3982-3986.

Panic, V.V., S.I. Seslija, A.R. Nesic and S.J. Velickovic, 2013. Adsorption of azo dyes on polymer materials. Hem. Ind., 67: 881-900.

Prosser, A.J. and E.I. Franses, 2001. Adsorption and surface tension of ionic surfactants at the air-water interface: Review and evaluation of equilibrium models. Colloids Surf. A. Physicochem. Eng. Aspects, 178: 1-4.

Robinson, R.A. and R.H. Stokes, 1968. Electrolyte Solutions. 2nd Edn., Butterworth's, London, USA., Pages: 590.

Sanghi, R. and B. Bhattacharya, 2002. Review on decolorisation of aqueous dye solutions by low cost adsorbents. Color Technol., 118: 256-269.

Shen, D., J. Fan, W. Zhou, B. Gao and Q. Yue *et al*., 2009. Adsorption kinetics and isotherm of anionic dyes onto organo-bentonite from single and multisolute systems. J. Hazard. Mater., 172: 99-107.

Siegrist, A.E., C. Eckhardt, J. Kaschig and E. Schmidt, 1991. Optical Brighteners. In: Ullmann's Encyclopedia of Industrial Chemistry, Properties, Applications, Hunger, K. (Ed.). Wiley-VCH, Weinheim, Germany, pp: 153-176.

Tara-Lunga-Mihali, M., N. Plesu, A. Kellenberger and G. Ilia, 2015. Adsorption of an azo dye on polyaniline/niobium substrate. Intl. J. Electrochem. Sci., 10: 7643-7659.

Zlem, C. and B. Demet, 2000. Adsorption of some textile dyes by hexadecyl trimethyl ammonium bentonite. J. Turk. Chem., 25: 193-200.